PCCP

PAPER

Cite this: *Phys. Chem. Chem. Phys.*, 2018, **20**, 2724

KL double core hole pre-edge states of HCl

D. Koulentianos,[ab] R. Püttner,[c] G. Goldsztejn,[bd] T. Marchenko,[be] O. Travnikova,[be] L. Journel,[be] R. Guillemin,[be] D. Céolin,[e] M. N. Piancastelli,[bf] M. Simon[be] and R. Feifel*[a]

Received 22nd June 2017,
Accepted 11th December 2017

DOI: 10.1039/c7cp04214k

rsc.li/pccp

The formation of double core hole pre-edge states of the form $1s^{-1}2p^{-1}(^{1,3}P)\sigma^*,n\ell$ for HCl, located on the binding energy scale as deep as 3 keV, has been investigated by means of a high resolution single channel electron spectroscopy technique recently developed for the hard X-ray region. A detailed spectroscopic assignment is performed based on *ab initio* quantum chemical calculations and by using a sophisticated fit model comprising regular Rydberg series. Quantum defects for the different Rydberg series are extracted and the energies for the associated double core hole ionization continua are extrapolated. Dynamical information such as the lifetime width of these double-core-hole pre-edge states and the slope of the related dissociative potential energy curves are also obtained. In addition, $1s^{-1}2p^{-1}V^{-1}n\ell\lambda n'\ell'\lambda'$ double shake-up transitions and double core hole states of the form $1s^{-1}2s^{-1}(^{1,3}S)\sigma^*,4s$ are observed.

I. Introduction

Electronic states in atoms and molecules where two inner shell electrons are simultaneously removed, resulting in the creation of double core holes (DCH), were discussed in a seminal paper by Cederbaum *et al.*[1] more than 30 years ago. As it was shown in this work, in the case of molecules, DCH created on the same atomic site, referred to as single site (ss) DCH are expected to exhibit greater orbital relaxation effects than the single core holes (SCH). Furthermore, DCH where the two vacancies have been created on different atomic sites, referred to as two site (ts) DCH, were predicted to exhibit more sensitive chemical shifts than the SCH, having the potential to substantially improve the well known technique of Electron Spectroscopy for Chemical Analysis (ESCA).[2]

DCH states can be formed either by simultaneously removing the two core electrons of the molecule which are, in what follows, referred to as DCH continuum states, or by a simultaneous core-ionization core-excitation mechanism,[3–10] which are, for brevity, referred to as DCH pre-edge states. In a simplified picture with just two active electrons the latter type of states can be thought of being formed in two different ways upon absorption of a single photon.[10] Either one of the two core electrons is ejected into the continuum by the interaction with a photon while the second electron is "shaken up" into an unoccupied valence orbital by a monopole transition (direct shake), or one of the two core electrons is excited into an unoccupied valence orbital in a dipole transition while the second core electron is "shaken off" (conjugate shake). A proper theoretical description of these processes has recently been given by Carniato *et al.*[11]

From an experimental point of view, DCH states have recently been observed using both synchrotron radiation (SR) and X-ray free electron lasers (XFEL).[12,13] Specifically Eland *et al.*[3] observed the formation of DCH states of NH_3 and CH_4, using a time of flight (TOF) magnetic bottle spectrometer allowing for multiple electron detection in coincidence. In this work both 1s electrons were ejected and the lowest double core ionization potential (DIP) could be determined from the measured kinetic energies of the two photoelectrons. Furthermore, the main decay path of such states, which is the ejection of two Auger electrons, was determined. Also, a first glimpse on DCH pre-edge states was obtained. Around the same time, Lablanquie and coworkers[6] presented similar studies on N_2, CO, CO_2 and O_2. Building on the works of Eland *et al.*[3] and Lablanquie *et al.*,[6] Püttner *et al.*[8] and Goldsztejn *et al.*[9] showed more recently that DCH states of the pre-edge type can also be observed using a high resolution single-channel electron spectroscopy technique for detecting the one core electron which gets ejected into the continuum at a very well defined kinetic energy. With this technique they were able to detect DCH states with binding energies up to 3.5 keV. In particular,

[a] *Department of Physics, University of Gothenburg, Origovägen 6B, SE-412 96 Gothenburg, Sweden. E-mail: raimund.feifel@physics.gu.se*
[b] *Sorbonne Universités, UPMC Univ. Paris 06, CNRS, UMR 7614, Laboratoire de Chimie Physique-Matière et Rayonnement, F-75005 Paris Cedex 05, France*
[c] *Fachbereich Physik, Freie Universität Berlin, Arnimallee 14, D-14195 Berlin, Germany*
[d] *Max-Born-Institut, Max-Born-Straße 2A, 12489 Berlin, Germany*
[e] *Synchrotron SOLEIL, L'Orme des Merisiers, Saint-Aubin, BP 48, F-91192 Gif-sur-Yvette Cedex, France*
[f] *Department of Physics and Astronomy, Uppsala University, Box 516, SE-751 20 Uppsala, Sweden*

in the work of Püttner *et al.*,[8] the formation of DCH states of the form $1s^{-1}2p^{-1}n\ell$ in Argon has been studied, and by applying a fit model and the Rydberg formula, the lowest ionization potential required for promoting the two core electrons into the continuum could be extrapolated. Similarly, Goldsztejn *et al.*[9] recorded the $1s^{-2}V$ DCH states in Ne and Feifel *et al.*[14] in CS_2 and SF_6, where V refers to the valence orbital of the excited electron.

Generally speaking, the coincidence method results in a more complete picture of the different types of DCH processes including, in a highly selective way, information on the associated decay pathways. In contrast, the single-channel electron spectroscopy technique applied in the present work has advantages for the study of cationic DCH pre-edge states for which only one of the two core electrons can be detected, because it is, from a technical point of view, more straight forward and because it offers a potentially higher kinetic energy resolution especially for high electron kinetic energies. The latter also implies in practice the possibility to extract information on the lifetime broadening of this type of DCH states,[8,9] provided that a sufficiently narrow photon energy bandwidth can be used for the investigation.

In the present work the formation of DCH pre-edge states of the forms $1s^{-1}2p^{-1}\sigma^*,n\ell$ and $1s^{-1}2s^{-1}\sigma^*,4s$ are studied for the HCl molecule, which is isoelectronic to the Ar atom, by using the same technique as in ref. 8 and 9. The atomic orbital notation used here relates to the fact that the core orbitals can be regarded as localized mainly on the Cl atom. The identification of the peaks observed is based both on a fit model used to reproduce the experimental electron spectrum, as well as on *ab initio* quantum chemical calculations.

II. Experimental details

The measurements were carried out at the French national synchrotron radiation facility SOLEIL in Paris, at the GALAXIES beam line,[15] where a dedicated hard X-ray photoelectron spectroscopy (HAXPES) end station is routinely available.[16] Briefly, in this set-up electrons are removed from the sample enclosed in a gas cell upon the impact of linearly polarized X-rays, provided by the U20 undulator of this storage ring. In order to select different photon energies, a Si(111) double crystal monochromator is used, along with a collimating mirror, which either has palladium or carbon coating, depending on the photon energy chosen. The ejected electrons are collected and analyzed by an EW4000 VG Scienta hemispherical analyzer, the lens of which is set parallel to the polarization direction of the X-rays. This spectrometer has a 60° acceptance angle.

In order to obtain reliable electron energies, calibration of the spectrometer was performed using known Ar LMM Auger lines. The binding energies used for calculating the kinetic energies of the Auger electrons were 248.63 eV[17] for Ar $2p_{3/2}{}^{-1}$ and 47.51 eV for Ar $3p^{-2}(^1D_2)$.[18] Subsequently, the known Ar 1s photoelectron line[19] was used for calibrating the selected photon energies, resulting in an accuracy of 0.4 eV for the binding energies due to the error of 0.3 eV for the Ar 1s binding energy.

HCl gas was commercially obtained with a stated purity of better than 99.5%. The purity of the sample was verified on-line by conventional core level spectroscopy.

III. Theoretical details

Ab initio quantum chemical calculations have been performed to support the assignment of the experimentally observed spectral features. Excitations of electrons to unoccupied valence and Rydberg orbitals were calculated using the Multi-Configuration Self Consistent Field (MCSCF) method, together with Dunning's augmented correlation consistent polarized core valence triple zeta (aug-cc-pCVTZ) basis set. The equilibrium internuclear distance for the neutral ground state of the HCl molecule was set to 1.274 Å.[20] The calculations were performed with the MOLPRO2015 quantum chemistry software.[21] For the $1s^{-1}2p^{-1}$ and $1s^{-1}2s^{-1}$ DCH states excitation energies to LUMO as well as to the Cl 4s Rydberg orbital have been calculated. By default, MOLPRO does not handle the molecule as belonging to the $C_{\infty v}$ point group. Therefore HCl was considered as belonging to C_{2v} point group. The active space consisted of 7 a_1, 3 b_1, 3 b_2 and 1 a_2 orbitals. Further expansion of the active space, which was practically not possible within the framework of the present work, is expected to reduce the apparent systematic deviation between the theoretical and experimental values.

IV. Results and discussion

A. Formation of $1s^{-1}2p^{-1}$ DCH states

Fig. 1 shows an experimental electron spectrum of HCl in the region of the Cl $1s^{-1}2(s,p)^{-1}$ shake-up satellites recorded at the photon energy of 3900 eV. The spectrum shows several intense

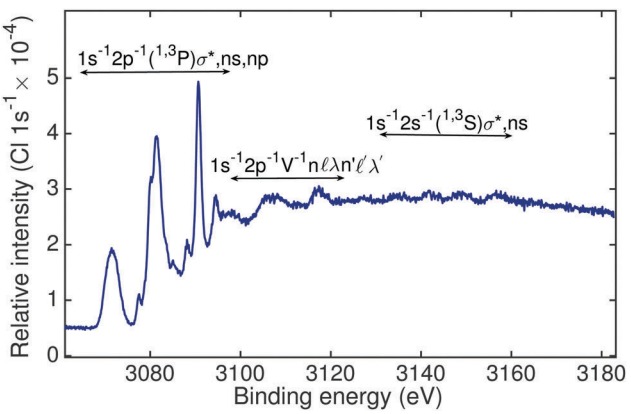

Fig. 1 Overview photoelectron spectrum of HCl, recorded at the photon energy of 3900 eV. Given are relative intensities in units of 10^{-4} times the intensity of the Cl $1s^{-1}$ main line. In the energy region below 3100 eV the $1s^{-1}2p^{-1}(^{1,3}P)\sigma^*,n\ell$ shake-up satellites are observed. From about 3130 eV on $1s^{-1}2s^{-1}(^{1,3}S)\sigma^*,4s$ states are visible. In addition, double shake-up states of the form $1s^{-1}2p^{-1}V^{-1}n\ell\lambda n'\ell'\lambda'$, where V refers to the 4σ, 5σ and 2π molecular orbitals, are present in the region between 3095–3130 eV.

Table 1 Theoretical and experimental energy values for the $1s^{-1}2p^{-1}(^{1,3}P)\sigma^*,n\ell$ and $1s^{-1}2s^{-1}(^{1,3}S)\sigma^*$,4s DCH states. The calculations were performed with the MCSCF method and by using the aug-cc-pCVTZ basis set. The double ionization potentials, DIP, are also given. The relative energy positions are expected to be correct within 50 meV while the entire binding energy scale is subject to an error of 0.4 eV due to the calibration procedure

	Theory (eV)	Exp. (eV)			Theory (eV)	Exp. (eV)
$1s^{-1}2p^{-1}$	^3P	$^3P_2$	$^3P_1$	$^3P_0$		$^1P_1$
σ*	3076.50	3071.07	3072.37	3073.42	3084.63	3081.72
4s	3083.00	3077.43	3078.73	3079.78	3091.23	3088.08
4p	—	3080.08	3081.38	3082.43	—	3090.73
5s	—	3083.11	3084.41	3085.46	—	3093.76
5p	—	3083.81	3085.11	3086.16	—	3094.46
6p	—	3085.26	3086.56	3087.61	—	3095.91
DIP	—	3087.99 ± 0.25	3089.29 ± 0.25	3090.34 ± 0.25	—	3098.64 ± 0.25

	$^3S_1$		$^1S_0$	
$1s^{-1}2s^{-1}$	Theory (eV)	Exp. (eV)	Theory (eV)	Exp. (eV)
σ*	3138.70	3134.66	3152.06	3148.83
4s	3145.58	3141.66	3159.07	3156.54
DIP	—	3151.91 ± 0.35	—	3166.43 ± 0.70

structures in the lower binding energy region, accompanied by weaker structures in the higher binding energy region. To get a first idea on the possible assignment of the observed features, we make use of the MCSCF calculations, yielding the results collated in Table 1. We note, that more precise calculations taking into account spin–orbit interaction might be worth carrying out in the future.

The features up to about 3100 eV binding energy are related to $1s^{-1}2p^{-1}(^{1,3}P)\sigma^*,n\ell$ transitions, whilst the features higher than 3130 eV binding energy are related to $1s^{-1}2s^{-1}(^{1,3}S)\sigma^*$,4s transitions. Generally speaking, according to Hund's rules, the $1s^{-1}2p^{-1}(^3P)$ states are expected to appear at lower binding energies than the associated $1s^{-1}2p^{-1}(^1P)$ states, as it was found in the isoelectronic Ar case study of Püttner *et al.*[8] In what follows we will give a more detailed assignment of the lower binding energy part of the spectrum by using a fit model based on physical arguments, which allows us to acquire information on the nature of the observed peaks.

The results of our fit model, which covers the lower binding energy part up to 3100 eV, are displayed in Fig. 2. Akin to the work of Püttner *et al.*,[8] where the $1s^{-1}2p^{-1}n\ell$ photoelectron spectrum of Ar was found to resemble a $1s^{-1}$ photoabsorption spectrum, we expect for the case of HCl[22] Rydberg states close to threshold and states connected with excitations into the σ* valence orbital in the lower energy region, where the latter is also cooperated by our MCSCF calculations.

Since exchange and spin–orbit splitting results for the $1s^{-1}2p^{-1}$ configuration in four different ionization thresholds ($^3P_{2,1,0}$,$^1P_1$), 16 strongly overlapping transitions are expected to be present in the energy region between 3076 and 3088 eV. In order to account for all these possible resonances we used a complex fit model in which the following aspects were included:

(1) We assume a fixed splitting between the different parent states for all excitations, in order to reduce the number of free parameters in the strongly overlapping region. A justification for this assumption has been given in the supplemental material provided in the work of Püttner *et al.*[8] The main drawback of this assumption is that any small variation in the term values of an excited state orbital relative to the corresponding ionization thresholds results in a loss of accuracy for the intensities; however, without this assumption there would have been too many free parameters for a meaningful fit.

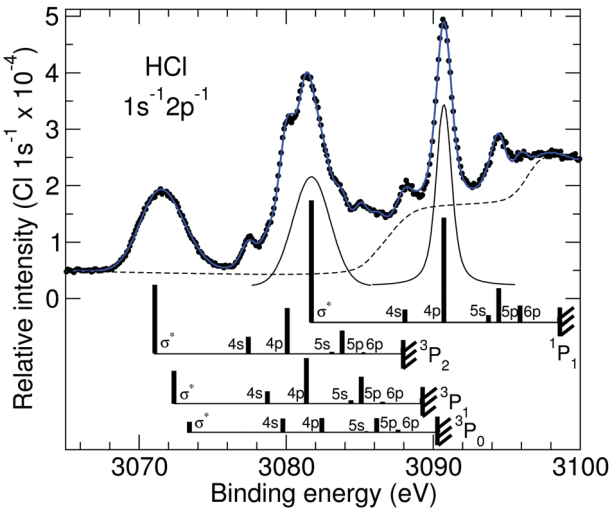

Fig. 2 The photoelectron spectrum of HCl in the region of the $1s^{-1}2p^{-1}$ excitations. Given are relative intensities in units of 10^{-4} times the intensity of the Cl $1s^{-1}$ main line. The blue solid line through the data points represents the fit results. The dashed line indicates the background comprising four arctan-functions and contributions of double shake-up states, while the solid line at 3081.5 eV and 3090.5 eV mimics the line shapes used in the fit analysis for the $1s^{-1}2p^{-1}\sigma^*$ and $1s^{-1}2p^{-1}n\ell$ excitations, respectively. The vertical-bar diagrams in the lower part indicate the energy positions and intensities obtained from this fit analysis.

(2) Regarding the line shapes describing the observed peaks, a Gaussian line shape, with a full width at half maximum (FWHM) of $\sigma \cong 4.13$ eV, has been used to model the excitations to σ* since these states are strongly dissociative and are expected to be quite broad, in agreement with our

experimental observation. In contrast, the Rydberg states are described well using a Lorentzian profile with a width of ≅630 meV (FWHM). This value is close to the calculated Cl $1s^{-1}$ lifetime width of 0.64 eV[23] which is expected to be also a good approximation for the Cl $1s^{-1}2p^{-1}$ DCH states as discussed in Püttner *et al.*[8] Obviously, the lifetime broadening is the dominant factor for the lineshape of these peaks, *i.e.* possible modifications caused by the nuclear motion are weak. From this we conclude that these Rydberg states are either bound or only weakly dissociative.

(3) The background is described by a linear function as well as an arctan function for each of the four Cl $1s^{-1}2p^{-1}$ ionization thresholds.[24] These arctan functions are located approximately 2 eV below the corresponding ionization threshold and are used to describe the unresolved higher-*n* Rydberg states as well as the continuum states. The mathematical form of the arctan function is due to the convolution of a step function describing the intensity with a Lorentzian function of 630 meV taking the lifetime broadening into account. In Fig. 2 only two distinct steps can be seen. As the three thresholds of triplet multiplicity are very close in energy, the energy positions of the steps are also very close in energy and the three arctan functions cannot be observed individually due to the lifetime broadening.

(4) Finally, the entire spectrum has been convoluted with a Gaussian of 585 meV (FWHM) to simulate the experimental resolution including photon bandwidth, detector resolution and Doppler broadening.

Based on this fit model, the very first peak around 3071 eV is associated with $1s^{-1}2p^{-1}(^3P_{2,1,0})\sigma^*$ transitions, which strongly overlap. This assignment is in good agreement with the present calculations that predict the $1s^{-1}2p^{-1}(^3P_{2,1,0})\sigma^*$ transitions as those with the lowest excitation energies, namely at ≅3076 eV. It is also fully in line with the observed Gaussian lineshape, see above, due to the strongly dissociative character of these states. In more detail, the slope of the potential energy curve of the corresponding DCH state X_{slope} can be derived on the basis of the Condon reflection approximation.[25] For this, the relation $X_{\text{slope}} = a\sigma$ can be employed. Here, σ is the width of the Gaussian function and $a^2 = \frac{\mu\omega}{\hbar}$, with μ being the reduced mass of the HCl molecule and ω the vibrational frequency.[26] In this way we obtained for the dissociative potential energy curve of the $1s^{-1}2p^{-1}\sigma^*$ DCH state at the equilibrium distance of the ground state a slope of $X_{\text{slope}} = -16.3(1.0)$ eV Å^{-1}. Here the 1.0 eV stands for the statistical errors of the fit analysis. In addition to this statistical error there is a systematic error based on the fact that the LUMO is described with a Gaussian function alone. As described above, the Gaussian function accounts for the overlap of the vibrational wavefunctions in the ground and the excited state. However, to account for the lifetime broadening this Gaussian function has to be convoluted with a Lorentzian function of a width of 630 meV. This has been omitted in the fit analysis due to technical reasons. From simulations we estimated this error to 1.2(0.3) eV Å^{-1} so that we finally result in a slope of $X_{\text{slope}} = -15.1(1.3)$ eV Å^{-1}. This value agrees quite well with the theoretical slope of $X_{\text{slope}} = -12.9$ eV Å^{-1} obtained in the present calculations, as well as with the value of $X_{\text{slope}} = -14.5$ eV Å^{-1} calculated in Travnikova *et al.*[27] for the case of $2p^{-2}\sigma^*$ DCH states in HCl. Here we want to point out that the slopes of the DCH states $1s^{-1}2p^{-1}\sigma^*$ and $2p^{-2}\sigma^*$ are expected to be similar. This is due to the fact that in both cases the excited electron experiences two strongly localized core holes, which have on the scale of the spatially extended excited state orbital a similar spatial distribution.

The $1s^{-1}2p^{-1}(^1P_1)\sigma^*$ contributes substantially at ≅3082 eV where it strongly overlaps with allowed Rydberg states within the triplet term. Also many of the triplet states associated with the different fine structure terms strongly overlap with each other. These states have been disentangled after reproducing the spectrum with the fit model. Regarding the assignment of the structures proposed so far, beyond the fit values given in Table 1, intensity arguments can be used in order to identify and separate the *n*s from the *n*p excitations.

Akin to the work of Püttner *et al.*,[8] after 1s ionization the 2p electron can only be excited to an *n*p unoccupied Rydberg orbital on the grounds of monopole selection rules for shake transitions, and for the same reason 2p ionization will be accompanied by *n*s excitation only. Furthermore the former process, where the 1s electron has been ionized and the 2p electron has been excited is expected to appear as a more intense process in the experimental electron spectrum. This can be understood by considering the nuclear charge felt by the core electron excited by the shake process. In the case of 1s ionization, the nuclear charge felt by the 2p electron changes significantly, as the screening of the 2p electron by the 1s is much stronger than the screening of the 1s electron by the 2p. As a result, the radial distribution of the 2p electron in the core-ionized state will differ significantly from the one in the ground state, giving rise to a strong shake-up effect. In contrast, ionization of a 2p electron will have a limited impact on the nuclear charge felt by a 1s electron, resulting in a small shake-up effect. Thus, excitations to *n*s Rydberg orbitals will appear as lower intensity peaks. In addition, the observed intensities can be understood in terms of the cross section of the 1s ionization, which at the used photon energy is much higher than the one corresponding to 2p ionization. The complete peak assignment is graphically included in Fig. 2.

We want to note that Yarzhemsky and Amusia[28] suggested for Argon in the region of the $1s^{-1}2p^{-1}4s$ excitations also contributions of the form $1s^{-1}2p^{-1}3d$ caused by knock-up. Although the data analysis of the Argon spectrum in ref. 8 shows no clear evidence of such contributions, they cannot be excluded and may also contribute in the present case of HCl. Clarifying the possible presence of these knock-up processes in $1s^{-1}2p^{-1}$ spectra can be an aim of future investigations.

With this peak assignment at hand, the DIPs as well as the quantum defects can be estimated from the well-known energy expression of Rydberg states, namely

$$E_n = \text{DIP} - \frac{Z^2 \cdot R}{(n - \delta_\ell)^2}, \quad (1)$$

where R is the Rydberg constant, E_n is the energy of the state observed and δ_ℓ is the quantum defect.

In the present case of DCH states the excited Rydberg electron experiences a nuclear charge of $Z = +2e$ so that the Rydberg constant has to be multiplied by 4. For determining the quantum defects and the DIP values from eqn (1) we make use of the common assumption that the quantum defect is approximately the same for states involving orbitals of the same orbital angular momentum ($n\ell$,$n'\ell$, *etc.*). Thus by fitting the energies of the $1s^{-1}2p^{-1}(^{1,3}P)ns$ states and the energies of $1s^{-1}2p^{-1}(^{1,3}P)np$ states to eqn (1) the quantum defects of the ns and np Rydberg series as well as the corresponding DIP values could be determined. The DIP value for each term is given in Table 1. We also note that for all terms considered we found that ns Rydberg electrons had a quantum defect $\delta_s = 1.76$ and np Rydberg electrons had a quantum defect $\delta_p = 1.35$. The error in the estimation of the quantum defects is ± 0.02 for both cases.

B. Formation of $1s^{-1}2s^{-1}$ DCH states

What concerns the high binding energy part of the spectrum above 3130 eV, the features observed are related to the formation of DCH states of the form $1s^{-1}2s^{-1}\sigma^*,4s$ as suggested by our calculations. In particular four distinct peaks are seen in Fig. 3 which correspond to excitations to the LUMO and to the 4s Rydberg orbital, respectively. The equal energy spacing assumption used before applies in this energy region, as the energy spacing between the peaks corresponding to σ* excitations in the triplet and singlet term is almost the same as the spacing between the peaks corresponding to 4s Rydberg excitations of the same multiplicity. Beyond the results of the calculations, the assignment of these peaks can be supported based on term values. In case of the $1s^{-1}2p^{-1}V$ DCH states the term value of the orbital V = σ* and V = 4s amounts 16.92 eV and 10.56 eV, respectively (see above). From the resonant KLL Auger spectra of HCl leading to the final states $2p^{-2}V$, the term values are derived to be 16.85 eV and 10.31 eV for the σ* and 4s Rydberg orbital, respectively.[29] These term values are similar because of the same argument used before for the slopes of the states $1s^{-1}2p^{-1}\sigma^*$ and $2p^{-2}\sigma^*$. By assuming a similar behavior for the $1s^{-1}2s^{-1}V$ states we expect a splitting of 6.5 eV between the $1s^{-1}2s^{-1}\sigma^*$ and the $1s^{-1}2s^{-1}4s$, in reasonable agreement with the fit result. Moreover, from these term values and the energy positions of the $1s^{-1}2s^{-1}\sigma^*,4s$ resonances the $1s^{-1}2s^{-1}(^{1,3}S)$ DIP can be extrapolated. Our results are given in Table 1.

C. Formation of double shake-up states

In the following we shall discuss the double-shake structures between 3095 eV and 3130 eV. Fig. 3 shows three intense and one weak pair of broad peaks split by ≅9 eV which corresponds to the splitting of the $1s^{-1}2p^{-1}(^{1,3}P)$ DIPs. These double shake-up states were not covered by the present calculations. To approach an assignment of these peaks in a first step we shall try to estimate the binding energies of the $1s^{-1}2p^{-1}(^{1,3}P)2\pi^{-1}$, $1s^{-1}2p^{-1}(^{1,3}P)5\sigma^{-1}$, and $1s^{-1}2p^{-1}(^{1,3}P)4\sigma^{-1}$ triple ionization

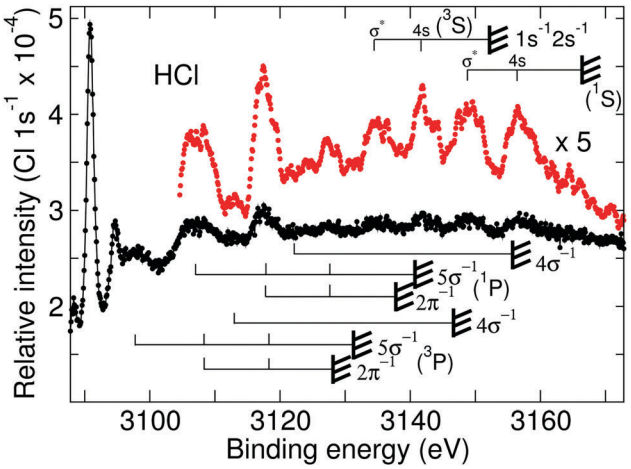

Fig. 3 Photoelectron spectrum in the energy region between 3088 eV and 3173 eV with the double shake-up region from 3088–3148 eV overlapping with the $1s^{-1}2s^{-1}$ shake regions in the range from 3137–3173 eV. Given are relative intensities in units of 10^{-4} times the intensity of the Cl $1s^{-1}$ main line. For the red data points the intensity is multiplied by a factor of five relative to the black data points. Moreover, for reasons of presentation the data represented by the red points are smoothed by averaging over neighbouring data points. For the assignment of the double shake-up states the estimated energy positions for the $1s^{-1}2p^{-1}(^{1,3}P)2\pi^{-1}$, $1s^{-1}2p^{-1}(^{1,3}P)5\sigma^{-1}$ and $1s^{-1}2p^{-1}(^{1,3}P)4\sigma^{-1}$ triple ionization thresholds are indicated below the spectrum, together with vertical bar diagrams for the observed peaks. The $1s^{-1}2s^{-1}\sigma^*,4s$ resonances and the corresponding ionization thresholds $1s^{-1}2s^{-1}(^{1,3}S)$ are indicated by the vertical bar diagrams above the spectrum. For more details, see text.

thresholds. From calculations performed in the present work we found the $1s^{-1}2p^{-1}2\pi^{-1}$, $1s^{-1}2p^{-1}5\sigma^{-1}$, and $1s^{-1}2p^{-1}4\sigma^{-1}$ triple ionization potentials 38.82 eV, 41.03 eV, and 56.45 eV above the corresponding DIP. These values are in reasonable agreement with those of the isoelectronic H_2S and Argon. For H_2S, the $2p^{-2}V^{-1}$ higher-n Ryd[1] states are found to be 31.5 eV above the corresponding $2p^{-2}$ states.[30] From this we conclude that the ionization potential of the valence orbitals in the presence of two core holes amounts at least 35 eV. An upper limit can be given using Argon and the Z+2 approximation. For the Z+2 atom for Ar, Ca^{2+}, an ionization energy of 50.91 eV for the 3p electron and 69.00 eV for the 3s electron can be found,[18] so that the present calculated values are well in between these two estimations representing lower and upper limits.

Based on the calculated ionization energies for the 2π, 5σ and 4σ valence electron as well as the experimental $1s^{-1}2p^{-1}(^{1,3}P)$ ionization energies the triple ionization potentials are estimated and indicated in Fig. 3. For this step, the spin–orbit splitting of the (^{3}P) states as well as any coupling between the DCH states and the vacancy in the valence shell is neglected.

In the following we shall discuss which double shake-up states are expected to be present in the spectrum. As mentioned above, in case of single shake up excitations the most intense states are $1s^{-1}2p^{-1}\sigma^*$ followed by $1s^{-1}2p^{-1}4p$ while all other states are of significantly less intensity. The valence shake-up accompanying the Cl 2p ionization in HCl is discussed by

Caravetta *et al.*[31] These authors found that the $2\pi^{-1}$ shake transitions are approximately 2 times more intense than the $5\sigma^{-1}$ shake transitions, *i.e.* it matches the atomic degeneracy ratio of the Cl 3p orbitals contributing to this molecular orbital. Moreover, it is found that the $4\sigma^{-1}$ shake transitions are considerably less intense.

In addition, Caravetta *et al.*[31] found that the 4σ and 5σ shake-up transitions start ≅14 eV below the shake-off threshold, while the 2π shake-up transitions start only ≅7 eV below the corresponding shake-off threshold. This finding can readily be explained by the fact that the monopole selection rules for shake processes allow $4\sigma \rightarrow \sigma^*$ and $5\sigma \rightarrow \sigma^*$, *i.e.* to the LUMO, while 2π shake-up processes all require a population of *n*p Rydberg states, which are higher in energy than the LUMO. The calculations of Caravetta *et al.*[31] also show that the shake probability is the highest for the lowest unoccupied orbitals, *i.e.* the LUMO as well as the low-*n* Rydberg orbitals.

By taking the above given arguments into account we expect that the most intense double shake-up states are $1s^{-1}2p^{-1}5\sigma^{-1}\sigma^{*2}$, $1s^{-1}2p^{-1}5\sigma^{-1}\sigma^{*1}4p\sigma^{1}$, $1s^{-1}2p^{-1}5\sigma^{-1}4p^{2}$, $1s^{-1}2p^{-1}2\pi^{-1}\sigma^{*1}4p\pi^{1}$, and $1s^{-1}2p^{-1}2\pi^{-1}4p^{2}$. From these the $1s^{-1}2p^{-1}5\sigma^{-1}\sigma^{*2}$ is expected to be the lowest in energy. By assigning the pair of peaks at ≅3098 eV and ≅3107 eV to the $1s^{-1}2p^{-1}(^{1,3}P)5\sigma^{-1}\sigma^{*2}$ states we result in a term value of ≅33 eV for the σ^{*2} orbitals, which is in good agreement with two times the term value of ≅16.9 eV for the σ* excited state orbital in the presence of a DCH, supporting the assignment. Interestingly, 15 eV higher a pair of weak peaks can be found. These two peaks possess a term value of ≅33 eV relative to the $1s^{-1}2p^{-1}4\sigma^{-1}$ triple ionization threshold, suggesting an assignment to $1s^{-1}2p^{-1}4\sigma^{-1}\sigma^{*2}$ based on the term value.

The pair of peaks at ≅3108 eV and ≅3118 eV is about 5 eV broad and has a term value of ≅20 eV relative to the $1s^{-1}2p^{-1}2\pi^{-1}$ triple ionization threshold and ≅22 eV relative to the $1s^{-1}2p^{-1}5\sigma^{-1}$ triple ionization threshold. Finally, one single peak can be found at ≅3128 eV, resulting in a term value of ≅10 eV and ≅12 eV relative to the $1s^{-1}2p^{-1}(^{1}P)2\pi^{-1}$ and $1s^{-1}2p^{-1}(^{1}P)5\sigma^{-1}$ triple ionization thresholds, respectively. An attribution to these two thresholds is supported by the fact that an attribution to the $1s^{-1}2p^{-1}(^{3}P)2\pi^{-1}$ and $1s^{-1}2p^{-1}(^{3}P)5\sigma^{-1}$ thresholds results in too low term values. Moreover, an attribution to the $1s^{-1}2p^{-1}(^{1,3}P)4\sigma^{-1}$ thresholds is in contradiction to the expected low intensity. The given assignment results in the $1s^{-1}2p^{-1}(^{3}P)2\pi^{-1}$ and $1s^{-1}2p^{-1}(^{3}P)5\sigma^{-1}$ components at 3118 eV and explains the relative high intensity of the peak at this energy position. With the term values for the $1s^{-1}2p^{-1}$ single shake-up states of ≅16.9 eV for the σ* orbital, ≅10.4 eV for the 4s orbital and ≅7.9 eV for the 4p, orbital and the assumption that the term values for the states with two electrons in exited state orbitals are approximately given by the sum of the individual term values the energy positions of the remaining double shake-up states of relevance can be calculated. In this way we obtain term values of ≅27 eV for the $1s^{-1}2p^{-1}5\sigma^{-1}\sigma^{*1}4s\sigma^{1}$ states, ≅24 eV for the $1s^{-1}2p^{-1}5\sigma^{-1}\sigma^{*1}4p^{1}$ and $1s^{-1}2p^{-1}2\pi^{-1}\sigma^{*1}4p^{1}$ states, as well as ≅16 eV for the $1s^{-1}2p^{-1}5\sigma^{-1}4p^{2}$ and $1s^{-1}2p^{-1}2\pi^{-1}4p^{2}$ states. Based on these term values the pair of peaks at 3108 eV and 3118 eV can be assigned to $1s^{-1}2p^{-1}5\sigma^{-1}\sigma^{*1}4s\sigma^{1}$ as well as the $1s^{-1}2p^{-1}5\sigma^{-1}\sigma^{*1}4p^{1}$ and $1s^{-1}2p^{-1}2\pi^{-1}\sigma^{*1}4p^{1}$ states. Finally, the peaks at 3118 eV and 3128 eV can be assigned to the $1s^{-1}2p^{-1}5\sigma^{-1}4p^{2}$ and $1s^{-1}2p^{-1}2\pi^{-1}4p^{2}$ states. The resulting term values are some eV lower than the above estimated values and may indicate that the calculated triple ionization thresholds are too low by the same value. However, all given assignments are only tentative and require confirmation by other methods and in particular by calculations.

V. Conclusions

By using a high resolution single channel electron spectroscopy technique recently developed for the hard X-ray region, DCH pre-edge states of the form $1s^{-1}2p^{-1}(^{1,3}P)\sigma^*,n\ell$ and $1s^{-1}2s^{-1}(^{1,3}S)\sigma^*,4s$ were investigated for the HCl molecule. Essential parts of the spectrum were interpreted by aid of *ab initio* quantum chemical calculations and by using a fit model which assumes regular Rydberg series. Quantum defects for the different Rydberg series have been extracted and the energies for the associated double core hole ionization continua were extrapolated. Dynamical information such as the lifetime width of these double-core-hole pre-edge states and the slope of the related dissociative potential energy curves were extracted. While the different fine structure terms within the triplet multiplicity (*i.e.* $^{3}P_{2,1,0}$) could not be fully resolved, a disentanglement of the different states within each fine structure term was still achieved with our fit model. In addition, double shake-up transitions have been observed in the medium binding energy part of the spectrum; these features are tentatively assigned.

Author contributions

M. S., M. N. P., R. P. and R. F. devised the research, D. K., R. P., G. G., T. M., O. T., L. J., R. G., D. C., M. N. P., and M. S. participated in the conduction of the experimental research, D. K. and R. P. performed the data analysis, D. K. and G. G. performed the theoretical calculations, D. K., R. P., M. N. P., M. S. and R. F. wrote the paper and all authors discussed the results and commented on the manuscript.

Conflicts of interest

There are no conflicts to declare.

Acknowledgements

This work has been financially supported by the Swedish Research Council (VR) and the Knut and Alice Wallenberg Foundation, Sweden. D. K. acknowledges financial support by Labex Michem, France. The experimental work was performed at the GALAXIES beam line of the synchrotron radiation facility SOLEIL, France (project no. 99150133), and the authors would like to thank the staff of SOLEIL for a smooth operation of the

facility. Dr Nicolas Sisourat is greatly acknowledged for discussions on the interpretation of the output files of MOLPRO.

References

1 L. S. Cederbaum, F. Tarantelli, A. Sgamellotti and J. Schirmer, *J. Chem. Phys.*, 1986, **85**, 6513.
2 *ESCA Applied to Free Molecules*, ed. K. Siegbahn, North-Holland, Amsterdam, 1970.
3 J. H. D. Eland, *et al.*, *Phys. Rev. Lett.*, 2010, **105**, 213005.
4 P. Linusson, *et al.*, *Phys. Rev. A: At., Mol., Opt. Phys.*, 2011, **83**, 023424.
5 P. Linusson, *et al.*, *Phys. Rev. A: At., Mol., Opt. Phys.*, 2013, **87**, 043409.
6 P. Lablanquie, *et al.*, *Phys. Rev. Lett.*, 2011, **106**, 063003.
7 P. Lablanquie, *et al.*, *Phys. Rev. Lett.*, 2011, **107**, 193004.
8 R. Püttner, *et al.*, *Phys. Rev. Lett.*, 2015, **114**, 093001.
9 G. Goldsztejn, *et al.*, *Phys. Rev. Lett.*, 2016, **117**, 133001.
10 M. Nakano, *et al.*, *Phys. Rev. Lett.*, 2013, **111**, 123001.
11 S. Carniato, *et al.*, *J. Chem. Phys.*, 2015, **142**, 014307.
12 F. Penent, *et al.*, *J. Electron Spectrosc. Relat. Phenom.*, 2015, **204**, 303.
13 N. Berrah, *et al.*, *Proc. Natl. Acad. Sci. U. S. A.*, 2011, **108**, 16912.
14 R. Feifel, *et al.*, *Sci. Rep.*, 2017, **7**, 13317.
15 J.-P. Rueff, *et al.*, *J. Synchrotron Radiat.*, 2015, **22**, 175.
16 D. Céolin, *et al.*, *J. Electron Spectrosc. Relat. Phenom.*, 2013, **190**, 188.
17 G. C. King, M. Tronc, F. H. Read and R. C. Bradford, *J. Phys. B: At. Mol. Phys.*, 1977, **10**, 2479.
18 NIST Atomic Spectra Database Levels Data.
19 M. Breinig, *et al.*, *Phys. Rev. A: At., Mol., Opt. Phys.*, 1980, **22**, 520.
20 NIST Chemistry WebBook.
21 H.-J. Werner, *et al.*, *MOLPRO, version 2015.1, a package of ab initio programs*.
22 S. Bodeur, *et al.*, *Z. Phys. D: At., Mol. Clusters*, 1990, **17**, 291.
23 M. O. Krause and J. H. Oliver, *J. Phys. Chem. Ref. Data*, 1979, **8**, 329.
24 *NEXAFS Spectroscopy, §7.3*, ed. J. Stöhr, Springer Series in Surface Science, 1992.
25 G. Herzberg, *Molecular Spectra and Molecular Structure I. Spectra of Diatomic Molecules*, Van Nostrand, New York, 1950, p. 392.
26 R. Püttner, *et al.*, *Phys. Rev. A: At., Mol., Opt. Phys.*, 2011, **83**, 043434.
27 O. Travnikova, *et al.*, *Phys. Rev. Lett.*, 2016, **116**, 213001.
28 V. G. Yarzhemsky and M. Ya. Amusia, *Phys. Rev. A*, 2016, **93**, 063406.
29 G. Goldsztejn, *et al.*, *Phys. Chem. Chem. Phys.*, 2016, **18**, 15133.
30 R. Püttner, *et al.*, *Phys. Rev. A*, 2016, **93**, 042501.
31 V. Carravetta, H. Ågren, D. Nordfords and S. Svensson, *Chem. Phys. Lett.*, 1988, **152**, 190.

